

Experimental Study of LCI Lasers Fabricated by Single MOCVD Overgrowth Followed by Selective Dopant Diffusion

Edward H. Sargent, D. A. Suda, *Member, IEEE*, A. Margittai, F. R. Shepherd, M. Cleroux, G. Knight, N. Puetz, T. Makino, *Senior Member, IEEE*, A. J. SpringThorpe, G. Chik, and J. M. Xu, *Senior Member, IEEE*

Abstract—We report the design, fabrication, and characterization of lateral current injection (LCI) lasers made using a single etch-and-regrowth followed by selective dopant diffusion. Devices are characterized electrically and optically from 10 to 300 K. Using the recently developed theory of the LCI laser, the threshold current, spontaneous efficiency, and stimulated efficiency are related to physical mechanisms that underlie the operation of this promising family of devices. We explore the prospects for LCI lasers to enable monolithic photonic integrated circuits and functional optoelectronic devices.

Index Terms—Integrated optoelectronics, semiconductor device fabrication, semiconductor device modeling, semiconductor epitaxial layers, semiconductor heterojunctions, semiconductor lasers.

I. INTRODUCTION

SEMICONDUCTOR lasers, in which current is injected laterally, have previously been recognized as promising candidates for enabling optoelectronic integration [1]–[7]. Functional optoelectronic devices, such as capacitively wavelength-tunable laser-transistors, have also been proposed, based on lateral injection [8]. By using the lateral direction, a degree of freedom little explored in conventional vertical injection devices, LCI lasers permit greater flexibility in electrical and optical design. In the LCI laser of Fig. 1—a low-chirp, directly modulated, high-speed laser—the vertical structure may be designed for maximum optical confinement, improved far-field, and high differential gain since the progress of laterally injected carriers is not impeded by high, thick, numerous barriers [8]. LCI lasers, by lending themselves to planar integration on semi-insulating material [5], permit reduced parasitic capacitance and facilitate interdevice isolation. The planar geometry lends itself naturally to microstrip transmission line interconnection [9]. Reduced chirp associated with free-carrier induced refractive index modulation is a further consequence of reduced doping near the active region.

LCI laser development has lagged behind vertical injection laser evolution because of a lack of theoretical investigation

Manuscript received June 26, 1998; revised July 15, 1998.

E. H. Sargent and J. M. Xu are with the Department of Electrical and Computer Engineering, University of Toronto, Toronto, ON M5S 1A4, Canada.

D. A. Suda, A. Margittai, F. R. Shepherd, M. Cleroux, G. Knight, N. Puetz, T. Makino, A. J. SpringThorpe, and G. Chik are with Nortel Technology, Nepean, ON K1Y 4H7, Canada.

Publisher Item Identifier S 1041-1135(98)07924-5.

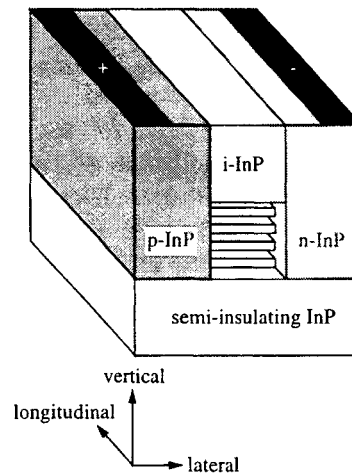


Fig. 1. High-speed LCI laser. Doping is minimal throughout the structure so that capacitance, free-carrier absorption, and chirp associated with free-carrier refractive index modulation are minimized. The vertical heterostructure—wells, barriers, confining heterostructures and cladding—may be optimized for maximum differential gain, without hampering even injection of carriers throughout the MQW active region.

and informed experimental exploration. Recent studies of LCI laser operation have revealed new effects central to LCI laser performance and unique to this class of lasers. These include the impact of ambipolar drift-diffusion in the presence of stimulated recombination [10]; the necessity of lateral carrier confinement even when injectors are separated by distances greater than the ambipolar diffusion length [11]; and the role of reduced active region series differential resistance in postponing the onset of current leakage through a parasitic path in parallel with the active region [12].

II. DESIGN AND PROCESSING

The epitaxial structure used in this investigation was grown on Fe:InP via low-pressure metal-organic chemical vapor deposition. Ten 55-Å undoped 1.5% compressively strained GaInAsP wells were clad by 200-Å 1.25Q p-doped ($8 \times 10^{17} \text{ cm}^{-3}$) barriers. This multi-quantum-well (MQW) active region (with room-temperature PL peak at 1585 nm) was clad above and below by *current guides* [6], 500-Å-thick layers of the same composition and doping as the barriers. This structure was sandwiched between 0.5- μm undoped InP cladding layers.

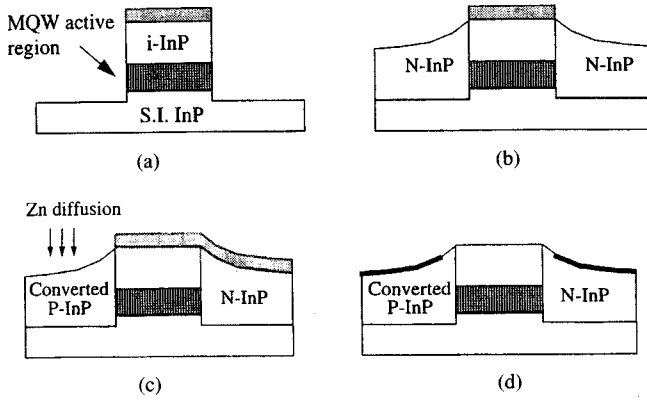


Fig. 2. Transverse cross section. Processing sequence for etched, regrown, and Zn-diffused type-converted LCI laser. (a) SiO_2 deposition and patterning; dry-etch InP-GaInAsP to below MQW. (b) N-type overgrowth. (c) Zn diffusion for selective type conversion. (d) Metallization.

By modeling the effect of ambipolar drift-diffusion of electrons and holes in the presence of stimulated recombination, it was found that a pronounced lateral carrier density nonuniformity will degrade the performance of LCI lasers by lessening the overlap between the fundamental lasing mode and the lateral gain profile [10]. This is aggravated above the lasing threshold: the carrier lifetime decreases as stimulated emission increases, the ambipolar diffusion length decreases, the nonuniformity of the carrier density increases, and the differential quantum efficiency decreases further. A number of remedies informed by these theoretical studies were incorporated into this structure.

- Compressively strained quantum wells were used to reduce the heavy-hole effective mass and increase thereby the mobility of the limiting carrier.
- Current guiding layers [6] and doped barriers were introduced for “hybrid” injection of carriers—predominantly lateral injection aided by some vertical carrier flow—into the active region. P-type guides were used to enhance injection of holes, the limiting carrier.
- Compressively strained quantum wells were also used in aid of reducing parasitic recombination effects (e.g., Auger recombination).
- Many quantum wells were used for a high-confinement factor low threshold carrier density. Parasitic effects (e.g., Auger recombination and carrier leakage) were thereby minimized.

The processing sequence is depicted in Fig. 2. Strong lateral carrier confinement, essential for high-performance operation, is achieved by etching followed by regrowth of a higher-bandgap material. Etch-and-regrowth trials on bulk InP material were used to achieve a planar morphology. In preparation for selective type conversion on one side of the ridge, patterning of the PECVD SiO_2 was followed by an O_2 plasma and an etch in dilute HF. Zinc diffusion was carried out at 450°C in a semi-sealed container using a solid zinc source.

III. RESULTS

A large voltage was required to pass current through the fully fabricated devices. Secondary ion mass spectroscopy

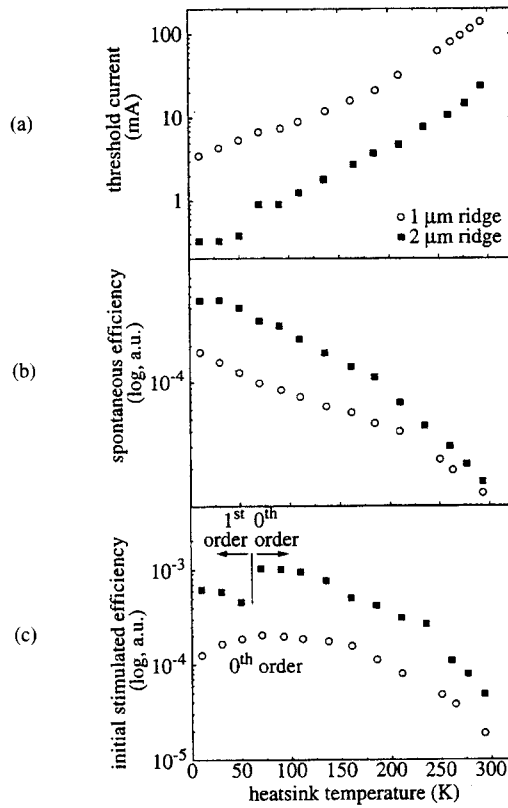


Fig. 3. Comparison of temperature evolution of measured: (a) threshold current, (b) spontaneous efficiency, and (c) stimulated efficiency with heatsink temperature under $1\text{-}\mu\text{s}/0.1\%$ pulsed excitation in 1- and $2\text{-}\mu\text{m}$ -wide active region devices.

(SIMS) revealed that the zinc diffusion front extended to a depth of $0.8\ \mu\text{m}$ (i.e., to the depth of the bottom quantum well). However, SIMS also revealed an unintended spike in the silicon doping level at the regrowth interface. The silicon doping spike, which reached a peak value of $3 \times 10^{19}\ \text{cm}^{-3}$, was not compensated during Zn diffusion of the future p-contact, resulting in a p-n-p-n structure. Because a large voltage was required to flatten this barrier, only pulsed-mode lasing was observed at room temperature. Furthermore, parallel leakage through the undoped cladding layers above and below the active region may be aggravated by the large voltage required to turn on the active region p-n-p-n electrical structure.

The dependence of threshold current, spontaneous efficiency, and stimulated efficiency are given in Fig. 3 for devices with 1- and $2\text{-}\mu\text{m}$ -wide ridges.

IV. DISCUSSION

First-order mode lasing may be favored over fundamental mode lasing in an LCI laser if the lateral gain profile is strongly nonuniform [7]. For this effect to account for the characteristic of Fig. 3(c), the threshold ambipolar diffusion length would have to drop to below its room temperature value at temperatures of $50\ \text{K}$ and below. The ambipolar diffusion length L may be written $L^2 = D\tau$, where the ambipolar diffusivity D is given by $D = (2D_n/1 + b)$, D_n is the electron diffusivity, the electron-hole mobility ratio b

is given by $b = \mu_e/\mu_h$, and μ_e and μ_h are the electron and hole mobility. In typical III-V semiconductors, b ranges from 10–20, so that $D \sim 2D_p$, where D_p is the hole diffusivity. If spontaneous emission dominates at threshold, the ambipolar diffusion length at the lasing threshold L_{th} may be written,

$$L_{th} \sim L_{th(\text{ref})} \sqrt{\frac{\mu_h(T)}{\mu_h(T_{\text{ref}})}} \quad (1)$$

where $L_{th(\text{ref})}$ is the ambipolar diffusion length at a reference temperature T_{Ref} .

The low-temperature hole mobility in GaInAsP drops below its room temperature value as ionized-impurity scattering becomes dominant at low temperatures [13]. From (1), the ambipolar diffusion length also drops below its room temperature value, the lateral gain nonuniformity becomes more severe, and lasing on the first-order mode is anticipated. The 1- μm -wide device exhibits consistent fundamental mode operation from 10 K to 300 K, with a continuous decrease in stimulated efficiency below 70 K. The overlap between the single-humped, laterally centered fundamental mode and the nonuniform, asymmetric lateral gain profile decreases as the ambipolar diffusion length drops at low temperatures.

Further confirmation of lateral gain nonuniformity is obtained by comparing the evolution of threshold current in 1- and 2- μm -wide devices [Fig. 4(a)]. The 2- μm device exhibits a discontinuous jump in the dependence of threshold current on heatsink temperature commensurate with switching between fundamental and first-order mode lasing; the 1- μm device exhibits a smooth temperature dependence.

To assess further the impact of diffusion of zinc into the active region, we obtained continuous-wave subthreshold electroluminescence spectra for a selection of devices. The spectral peak for the narrow active region device is shifted to a longer wavelength, and the spectrum of the narrow active region device is broader. We may explain these observations with reference to preferential intermixing of group-III sublattice atoms by diffused Zn, which causes a red-shift in the emission spectrum. In 1- μm -wide devices, much of the active region material may have been intermixed due to diffusion of Zn beneath the ridge, since the lateral diffusion distance is to be comparable to the vertical diffusion distance.

Two technological aspects require further improvement for this approach to LCI laser fabrication to result in high-performance, room-temperature, continuous-wave devices. The silicon spike at the regrowth interface must be reduced so that it may be compensated in the type-conversion process. Damage to and intermixing of the active region during type-conversion must also be reduced. This could be achieved by careful optimization of the two-dimensional diffusion of zinc in the doped heterostructure in question; or by implanting a nonintermixing, low-mass species such as beryllium for type conversion.

Lateral injection of current may aid in enabling functional optoelectronic devices—active optical sources with a non-

monotonic dependence of output on input, devices which exploit basic physical interactions in the semiconductor structure. The p-n-p-n device realized herein has the potential to act as a light-activated thyristor which could be switched between its on and off state by the application of an incident optical signal, possibly of a different wavelength. This device could act as an integrated optical switch or wavelength converter.

V. CONCLUSION

LCI lasers grown on semi-insulating substrates were fabricated using a single etch-and-regrowth step followed by selective dopant diffusion. This technique permits the formation of large, abrupt heterojunctions for strong lateral carrier confinement while simplifying processing by reducing the number of overgrowth steps. Further technological tailoring of key processes—preparation, regrowth, and type conversion—should enable the development of high-speed, low-chirp, integrable, functional lasers.

REFERENCES

- [1] H. Namizaki, H. Kan, M. Ishii, and A. Ito, "Transverse-junction-stripe-geometry double-heterostructure lasers with very low threshold current," *J. Appl. Phys.*, vol. 45, pp. 2785–2786, 1974.
- [2] K. L. Yu, U. Koren, T. R. Chen, and A. Yariv, "A groove GaInAsP laser on semi-insulating InP using a laterally diffused junction," *IEEE J. Quantum Electron.*, vol. QE-18, pp. 817–819, 1982.
- [3] S. K. Sargood, G. W. Taylor, P. R. Claisse, T. Vang, P. Cooke, D. P. Docter, P. A. Kiely, and C. A. Burrus, Jr., "A quantum-well inversion channel heterostructure as a multifunctional component for optoelectronic integrated circuits," *IEEE J. Quantum Electron.*, vol. 29, pp. 136–149, 1993.
- [4] A. Furuya, M. Makiuchi, O. Wada, T. Fujii, and H. Nobuhara, "Al-GaAs/GaAs lateral current injection (LCI)-MQW laser using impurity-induced disordering," *Jpn. J. Appl. Phys.*, vol. 26, pp. L134–L135, 1987.
- [5] K. Shimoyama, M. Katoh, Y. Suzuki, T. Satoh, Y. Inoue, S. Nagao, and H. Gotoh, "CW operation and extremely low capacitance of TJ-BH MQW laser diodes fabricated by entire MOVPE," *Jpn. J. Appl. Phys.*, vol. 27, pp. L2417–L2419, 1988.
- [6] K. Oe, Y. Noguchi, and C. Caneau, "GaInAsP lateral current injection lasers on semi-insulating substrates," *IEEE Photon. Technol. Lett.*, vol. 6, pp. 479–481, 1994.
- [7] E. H. Sargent, J. M. Xu, C. Caneau, and C. E. Zah, "Experimental investigation of physical mechanisms underlying lateral current injection laser operation," *Appl. Phys. Lett.*, vol. 73, no. 3, July 20, 1998.
- [8] E. H. Sargent, G. L. Tan, and J. M. Xu, "Physical model of OEIC-compatible lateral current injection lasers," *IEEE J. Select. Topics Quantum Electron.*, vol. 3, pp. 507–512, 1997.
- [9] D. A. Tauber, M. Horita, A. L. Holmes, Jr., B. I. Miller, and J. E. Bowers, "The microstrip laser," in *Proc. Integrated Photonics Research Top. Meet.*, 1996, vol. 6, pp. 533–536.
- [10] E. H. Sargent and J. M. Xu, "Investigation of the physical mechanisms governing the performance of OEIC-compatible p-i-n active region lateral injection lasers," presented at the IEEE Lasers and Electro-Optics Society (LEOS) 9th Annu. Meet., Nov. 1996.
- [11] ———, "Integration-compatible lateral current injection lasers: Design of 2-D heterostructure devices," presented at the Conf. Lasers and Electro-Optics (CLEO)/Pacific Rim, July 1997.
- [12] E. H. Sargent, K. Oe, C. Caneau, and J. M. Xu, "OEIC-enabling LCI lasers with current guides: Experimental investigation of internal operating mechanisms," *IEEE J. Quantum Electron.*, vol. 34, pp. 1280–1287, 1998.
- [13] J. R. Hayes, A. R. Adams, and P. D. Greene, "Low-field carrier mobility," in *GaInAsP Alloy Semiconductors*, T. P. Pearsall, Ed. New York: Wiley, 1982.